Journal of University of Science and Technology Beijing
Volume 12, Number 1, February 2005, Page 85

Materials

Investigations of high-frequency induction hardening process for piston rod of shock absorber

Xianhua Cheng and Qianqian Shangguan

School of Mechanical & Power Engineering, Shanghai Jiaotong University, Shanghai 200030, China
(Received 2004-02-17)

Abstract: The microhardness of piston rods treated with different induction hardening processes was tested. The experimental results reveal that the depth of the hardened zone is proportional to the ratio of the moving speed of the piston rod to the output power of the induction generator. This result is proved correct through the Finite Element Method (FEM) simulation of the thermal field of induction heating. From tensile and impact tests, an optimized high frequency induction hardening process for piston rods has been obtained, where the output power was 82%×80 kW and the moving speed of workpiece was 5364 mm/min. The piston rods, treated by the optimized high frequency induction hardening process, show the best comprehensive mechanical performance.

Key words: high-frequency induction hardening; piston rod; mechanical properties; finite element method; numerical simulation

1 Introduction

Shock absorbers play an important role in stability, safety and comfort for automobiles. Piston rods of shock absorbers are usually subjected to impact wear due to the intensive vibration after running for a long time. The wear of piston rods induces other mechanical failures such as noise, erosion and fatigue cracks.

Usually, piston rods are plated with chromium in order to prevent rigid friction and ensure better oil lubrication. From the failure analysis of piston rods, it was found that the chromium plating is usually torn and removed from the surface of piston rods due to immense impact loads [1]. In order to reduce the wear on the piston rods, enhancement of the bonding strength between the matrix and the chromium layer of piston rods is necessary. To achieve this, a better backing condition for the chromium layer should be provided.

The induction hardening process plays an important role in improving the backing condition of the chromium layer of piston rods. The usually required depth of the hardened zone for piston rods to obtain good mechanical properties of the piston rod matrix after undergoing the induction hardening process is 0.85 mm. However, it was found that the anti-abrasion properties of the piston rods with a depth of hardened zone of 0.8 mm, treated by current process, were not satisfactory. In order to improve the anti-abrasion properties and comprehensive mechanical properties of piston rods, it is necessary to adjust the parameters of the induction hardening process and thus to implement an optimization process.

The main factors affecting the induction hardening process include the current of the coil, the traverse speed of the specimen and the gap between the coil and the specimen [2-4], as well as modification of the inductor design [3]. In this study, the microhardness testing of piston rods treated with different induction hardening processes and the numerical simulation of thermal field of induction heating for piston rods were performed in order to find out the relationship among the depth of induction hardening, the output power of induction generators and the moving speed of piston rods. After the tensile and notch impact tests of the induction hardening treated piston rods, an optimized induction hardening process for piston rods was selected.

2 Research methods

The body material of the piston rod is 1035 steel and its diameter is 2.4 mm. A series of microhardness tests were done to find the relationship among the depth of the hardened zone, the ratio of the moving speed of the piston rod and the output power of the induction generator. The microhardness tests were performed on an AMH-100 fully automatic device. The testing environment is shown in **table 1**.

Table 1 Microhardness testing environments

Indenter	Press load /N	Lens magnification	Calibration / ($mm \cdot pix^{-1}$)
Vickers	9.8	40X	0.00036

Corresponding author: Xianhua Cheng, **E-mail:** xhcheng@sjtu.edu.cn

A finite element analysis software, ANSYS/Thermal, was used to simulate the thermal field for high-frequency induction hardening process.

Mechanical properties tests such as tensile and notch impact tests were applied to piston rods treated with different induction heating parameters in order to find out the optimum parameters of the induction process. Tensile and impact notch tests were performed on a CSS-1120 electronics omnipotent tester at 5 mm/min and on a JB-300J pendulum machine under the impact speed of 5.5 m/s respectively. The circumstance temperature of these tests was kept at (25±5)°C. The samples for both tests are shown in **figures 1** and **2**, respectively. Considering the point effect of surface hardening, U shape notch was used in impact notch test.

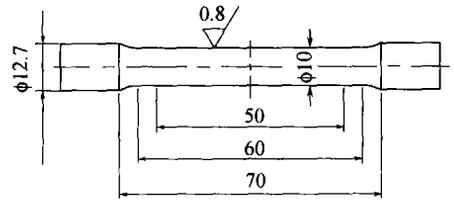

Figure 1 Sample of tensile test (unit: mm).

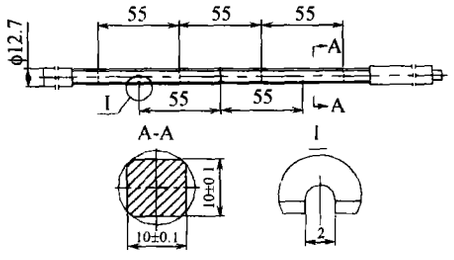

Figure 2 Sample of impact testing (unit: mm).

3 Results and discussion

3.1 Microhardness test

The depth of the hardened zone created by the induction hardening process should meet the requirements of manufacturing and should enhance the anti-abrasion properties of the piston rod. The required depth of the hardened zone is about 0.84 mm. If the depth of the hardened zone is too deep, there would be a dangerous tendency which overheating and excessive internal stress during the hardening process would be created. If the depth of the hardened zone is too shallow, it would be hard to meet the anti-abrasion requirement of the piston rod. Generally, the depth of the hardened zone is determined by the moving speed of the workpiece and the output power of the high-frequency induction generator [5].

In order to keep the depth of the hardened zone of piston rods at the required constant value, microhardness tests were done to find out the relationship between the moving speed and the output power. Five groups of parameters were selected as shown in **table 2**.

Table 2 Five groups of different induction hardening parameters

Sample No.	Output power of the generator / (%×80 kW)	Moving speed of the poiston rod / (mm·min^{-1})
1#	80	4500
2#	84	5100
3#	86	5400
4#	88	5900
5#	90	6100

The results of the microhardness tests under the environment of table 1 are shown in **table 3**. The depth of hardened zone where the value of microhardness is above HV400 was determined according to the data of table 3 by the interpolation method. **Table 4** shows the depths of the hardened zone at five different speed/power parameters. A linear relationship between the depth of hardened zone and the ratio of moving speed to output power of the induction generator (speed/power) was obtained as shown in **figure 3**. Therefore, if the ratio of the moving speed of the piston rods to the output power of the induction generator is kept constant, the same depth of the induction hardened zone will be obtained.

3.2 Thermal field FEM simulation of induction hardening for the piston rod

(1) Calculation model for the thermal field of surface high-frequency induction hardening.

The induction hardening process includes three stages: induction heating, water quenching and air cooling. The high frequency induced eddy current will generate a high surface power density during the induction heating stage. High-pressure water is sprayed onto the surface to be hardened for the piston rod during the water quenching stage, and a thin layer of warm water will remain on the surface of the piston rod during the air cooling stage. Actually, the induction hardening process is a progressive one, but an arbitrary cross-section of the piston rod will undergo all the three stages sequentially. The instantaneous calculation model for the induction hardening process of the piston rod is shown in **figure 4**.

The piston rod is made of 1035 steel, which is Ferro-magnetic material. During induction heating, a high density eddy current is induced by the exciting of alternating electromagnetic fields. The current is so powerful that the surface temperature goes up instantly to the Curie point (approximately 760°C), and

then, the value of relative permeability goes down to 1. Generally, the heating layer can be divided into two layers, the outer one loss magnetism and the internal one is out of the current penetration [6]. The peak of the power density lies between the internal and outer layers. According to the investigation, the peak will move inside continuously. Then, the induction hardening is transferred from the cold penetration stage where the skin depth of current penetration is smaller than the depth of the hardened zone to the hot penetration stage where the depth of current penetration is larger than the depth of the hardened zone. Finally, a balanced current penetration layer is generated, which can be determined by [7]

$$\delta_x = 500/\sqrt{f} \tag{1}$$

The induction frequency in this work is 250 kHz, and then the depth of the balance current penetration layer is 1 mm based on equation (1).

Table 3 Testing results of microhardness

1#		2#		3#		4#		5#	
Depth / mm	Hardness (Hv)	Depth / mm	Hardness (Hv)	Depth / mm	Hardness (Hv)	Depth / mm	Hardness (Hv)	Depth / mm	Hardness (Hv)
0.247	597	0.253	548	0.25	570	0.240	539	0.252	590
0.347	603	0.353	556	0.35	579	0.340	544	0.352	593
0.447	611	0.453	563	0.45	601	0.440	558	0.452	626
0.547	641	0.553	580	0.55	629	0.540	676	0.552	609
0.647	588	0.653	623	0.65	649	0.640	576	0.652	624
0.747	565	0.753	596	0.75	586	0.740	557	0.752	565
0.847	552	0.853	508	0.85	477	0.840	454	0.852	374
0.947	404	0.953	305	0.95	283	0.940	297	0.952	235
1.047	217	1.053	221	1.05	236	1.040	218	1.052	213
1.147	233	1.153	222	1.15	231	1.140	237	1.152	228

Table 4 Depth of hardened zone and speed/power under different parameters

Sample No.	Output power / (%×80 kW)	Moving speed / (mm·min^{-1})	(Speed/Power)/ (mm·min^{-1}·kW^{-1})	Depth of the hardened zone / mm
1#	80	4500	56.25	0.957
2#	84	5100	60.71	0.906
3#	86	5400	62.79	0.890
4#	88	5900	67.05	0.843
5#	90	6100	67.78	0.838

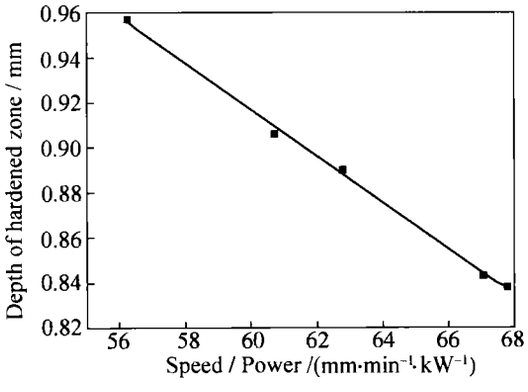

Figure 3 Linear fitting curve between the depth of the hardened zone and the speed/power.

The surface heat source density of the piston rod can be changed into volume heat source density in the current penetration layer due to the law of energy conservation. This is given by:

$$\int_\Omega q\mathrm{d}v = ps \tag{2}$$

where q is the volume heat source density, p is the surface heat source density, s is the area of the piston rod's heated surface.

After a balanced current penetration layer is established, *e.g.* 1 mm as determined by equation (1), as the induction frequency is 250 kHz, three separate zones can be estimated, which are corresponding to the current penetration zone, the transition zone and the core zone, respectively. The transition zone is an area where no current is generated, but it is still affected by the thermal conduction of the outer layer. The core zone is the area that is almost never affected by the induction heating process. Also, the magnetic leakage effect at the fringe of the coil must be considered. Therefore, the distribution of the heat source density can be expressed as shown in **figure 5**.

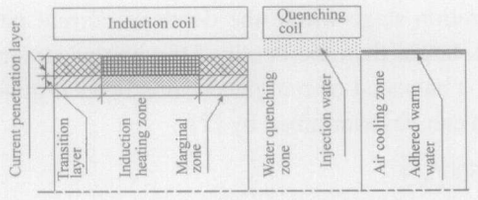

Figure 4 Instantaneous calculation model of surface high-frequency induction hardening of the piston rod.

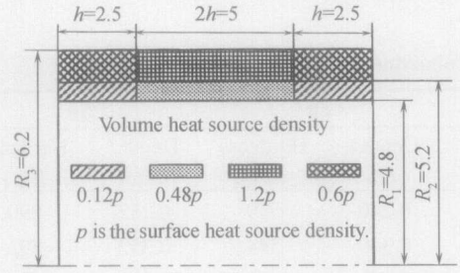

Figure 5 Diagram of heat source density distribution in the piston rod during surface induction hardening (unit: mm).

According to equation (2) the heat source in figure 5 can be calculated as following:

$$(Q_1+Q_2)\cdot\pi(R_3^2-R_2^2)\cdot 2h+(Q_3+Q_4)\cdot\pi(R_2^2-R_1^2)\cdot 2h=$$
$$p\cdot 2\pi r_3\cdot 4h \qquad (3)$$

where Q is the volume heat source density, R is the radius and, p the surface heat source density, which can be obtained by using a high frequency induction heating machine.

(2) Results of the simulation.

Two induction heating processes with the same speed/power, *i.e.* 67.05, were chosen as shown in **table 5**. The induction heating time and surface heat source density were determined by the induction heating machine.

The thermal fields of the piston rod treated by above two processes were simulated by ANSYS finite element analysis software. The simulation result is shown in **figure 6**.

Table 5 Heating time and surface heat source density of two different processes with the same ratio of speed/power

Processe No.	Output power / (%×80 kW)	Moving speed / (mm·min^{-1})	(Speed/Power) / (mm·min^{-1}·kW^{-1})	Heating time / s	Surface heat source density / (kW·mm^{-2})
1#	82	5498	67.05	0.1091	0.0396
2#	88	5900	67.05	0.1017	0.0419

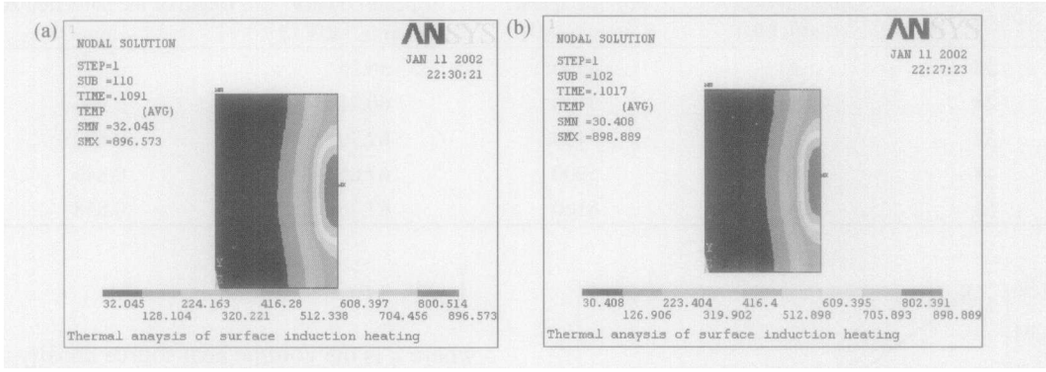

Figure 6 Results of the simulated thermal field of a piston rod treated by the processes shown in table 5: (a) 1# process; (2)2# process.

It can be seen from the simulation results that the thermal fields of piston rods treated by the above two processes are quite similar and the temperatures on the surface are almost the same.

It can be concluded that the temperature distribution during induction heating is directly in proportion to the ratio of speed/power. If the piston rods are treated by processes with the same speed/power, the thermal field would be the same. It is well known that the depth of the hardened zone will be the same if the steel components with the same heating temperature distribution are quenched down under the same cooling conditions. Therefore, the depth of the hardened zone of the piston rods are the same if the ratio of speed/power kept constant. The result of simulation verifies the experimental result obtained in section 3.1.

3.3 Process optimization and parameter adjustment

It is obvious that the optimization of the induction hardening process requires the adjustment of the moving speed of the piston rod and the output power of the induction generator. In order to keep the depth of the hardened zone at a perfect value, the ratio of speed/power should be kept constant during adjustment. Six groups of parameters under adjustment were

selected, shown in **table 6**, where the ratio of speed/power is 67.05 and the corresponding depth of the hardened zone is 0.84 mm.

Table 6 High-frequency induction hardening processes under the same value of speed/power

Process No.	Output power of the generator / (%×80 kW)	Moving speed of the piston rod / (mm·min^{-1})
1#	80	5364
2#	82	5498
3#	84	5632
4#	86	5766
5#	88	5900
6#	90	6034

A tensile test and an impact notch test were done for piston rods treated by the induction hardening processes under different parameters, to compare their comprehensive mechanical properties. Three samples of each process in table 6 were prepared and tested. The results of both tests are shown in **figure 7**.

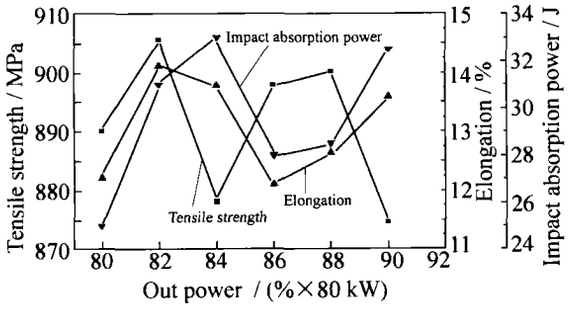

Figure 7 Mechanical properties of piston rods after different hardening processes.

It can be seen from figure 7 that the piston rod with a higher tensile strength has a relatively lower ductility. However the piston rod treated by the process with output power of 82%×80 kW has not only the highest tensile strength but also satisfactory ductility. It can be concluded that the piston rod treated by process No.2 in table 6 represents the best comprehensive mechanical property compared to piston rods treated by other processes. Therefore, process No.2 was chosen as the optimum process.

4 Conclusions

(1) Through the surface microhardness testing of piston rods treated by the induction hardening process, it was found that there is a linear relationship between the depth of the hardened zone and the ratio of moving speed to output power of the induction generator (speed/power).

(2) Results of FEM simulation for the thermal field of induction heating showed that the thermal fields of the piston rod treated by different processes, but with the same value of speed/power, are identical and the depths of hardened zones are the same after quenching at a same cooling rate.

(3) The piston rod treated by the optimized process, where the moving speed is 5498 mm/min and the output power is 82%×80 kW, represents the best comprehensive mechanical properties.

References

[1] X.H. Cheng, Y.J. Xue, and W.Z. Huang, Wear failure and fracture mechanics analysis of automobile absorber connection rod, *Tribology* (in Chinese), 21(2001), No.3, p.218.

[2] Lal Ch.Ch, Quality control of induction hardened cast iron cylinder head valve seats, *Mater. Sci. Forum*, 163(1993), No.6, p.367.

[3] H.T. Lee and D.J. Hwang, Study of the effect of induction surface hardening on AISI 1045 mild carbon steel, *J. Chin. Soc. Mech. Eng.* (in Chinese), 10(1989), No.5, p.365.

[4] K. Madler and J. Grosch, Einfluss des induktiven anlassens auf die biegefestigkeit randschichtgeharteter gefuge, *HTM-Haerterei-Technische Mitteilungen*, 56(2001), No.5, p.332.

[5] S.L. Semiation and D.E. Stutz, *Induction Heat Treatment of Steel*, Metals Park, Ohio:American Society for Metals, 1986, p.50-53.

[6] Z.R. Liu, *Induction Heat Treatment of Metals* (in Chinese), China Machine Press, Beijing, 1985, p.50.

[7] John Davies and Peter Simpson, *Induction Heating Handbook*, McGraw-Hill, London, 1979, p.254.